The F-BAR Cdc15 promotes contractile ring formation through the direct recruitment of the formin Cdc12

Alaina H. Willet,[1] Nathan A. McDonald,[1] K. Adam Bohnert,[1] Michelle A. Baird,[2,3] John R. Allen,[2,3] Michael W. Davidson,[2,3] and Kathleen L. Gould[1]

[1]Department of Cell and Developmental Biology, Vanderbilt University School of Medicine, Nashville, TN 37232
[2]National High Magnetic Field Laboratory and [3]Department of Biological Science, The Florida State University, Tallahassee, FL 32306

In *Schizosaccharomyces pombe*, cytokinesis requires the assembly and constriction of an actomyosin-based contractile ring (CR). Nucleation of F-actin for the CR requires a single formin, Cdc12, that localizes to the cell middle at mitotic onset. Although genetic requirements for formin Cdc12 recruitment have been determined, the molecular mechanisms dictating its targeting to the medial cortex during cytokinesis are unknown. In this paper, we define a short motif within the N terminus of Cdc12 that binds directly to the F-BAR domain of the scaffolding protein Cdc15. Mutations preventing the Cdc12–Cdc15 interaction resulted in reduced Cdc12, F-actin, and actin-binding proteins at the CR, which in turn led to a delay in CR formation and sensitivity to other perturbations of CR assembly. We conclude that Cdc15 contributes to CR formation and cytokinesis via formin Cdc12 recruitment, defining a novel cytokinetic function for an F-BAR domain.

Introduction

Cytokinesis is the terminal stage in cell division that results in the physical separation of two daughter cells. In many eukaryotic cells, an actomyosin-based contractile ring (CR) forms between the two segregated genomes and eventually constricts, dividing the mother cell into two daughter cells. In *Schizosaccharomyces pombe*, a powerful model organism for cytokinesis studies, assembly of the CR relies on a single formin, Cdc12, which is essential for nucleation and elongation of F-actin during CR formation (Nurse et al., 1976; Chang et al., 1997; Kovar et al., 2003; Kovar and Pollard, 2004) and also contributes to CR maintenance by bundling F-actin (Bohnert et al., 2013). Cdc12 recruitment to the medial cortex during CR formation relies on two redundant genetic modules (Wachtler et al., 2006; Laporte et al., 2011). Specifically, mutation of either IQGAP Rng2 or Myosin II in combination with the F-BAR (FER/Cip4 homology Bin–Amphiphysin–Rvs) scaffold Cdc15 eliminates Cdc12 recruitment to the division site and CR formation (Laporte et al., 2011). However, the mechanistic contributions of these genetic pathways are unknown.

Cdc15 is the founding member of the Pombe Cdc15 Homology family of proteins, which generally dimerize and bind membranes through their conserved N-terminal F-BAR domains (Tsujita et al., 2006) and interact with proteins though C-terminal protein-binding domains (Roberts-Galbraith and Gould, 2010). Although Cdc15 is essential for cytokinesis, it is unclear whether Cdc15's role in Cdc12 recruitment is important for CR assembly. Some studies reported that *cdc15* temperature-sensitive mutants lack CRs or produce them in only a fraction of cells (Fankhauser et al., 1995; Chang et al., 1996; Carnahan and Gould, 2003). Others found that cells lacking *cdc15* formed rings of F-actin at the cell middle during early stages of mitosis, but these rings were not maintained during anaphase, leading to the conclusion that CR formation per se is independent of Cdc15 (Balasubramanian et al., 1998; Arai and Mabuchi, 2002; Wachtler et al., 2006; Hachet and Simanis, 2008; Laporte et al., 2011; Arasada and Pollard, 2014). Given that Cdc15 defines one of two genetic pathways of formin recruitment (Laporte et al.,

Correspondence to Kathleen L. Gould: kathy.gould@vanderbilt.edu

K.A. Bohnert's present address is Dept. of Biochemistry and Biophysics, University of California, San Francisco, San Francisco, CA 94158.

Abbreviations used in this paper: CR, contractile ring; Lat-A, Latrunculin-A; MBP, maltose-binding protein; mNG, mNeonGreen; ROI, region of interest; SIN, septation initiation network; SPB, spindle pole body; YE, yeast extract.

The Rockefeller University Press $30.00
J. Cell Biol. Vol. 208 No. 4 391–399
www.jcb.org/cgi/doi/10.1083/jcb.201411097

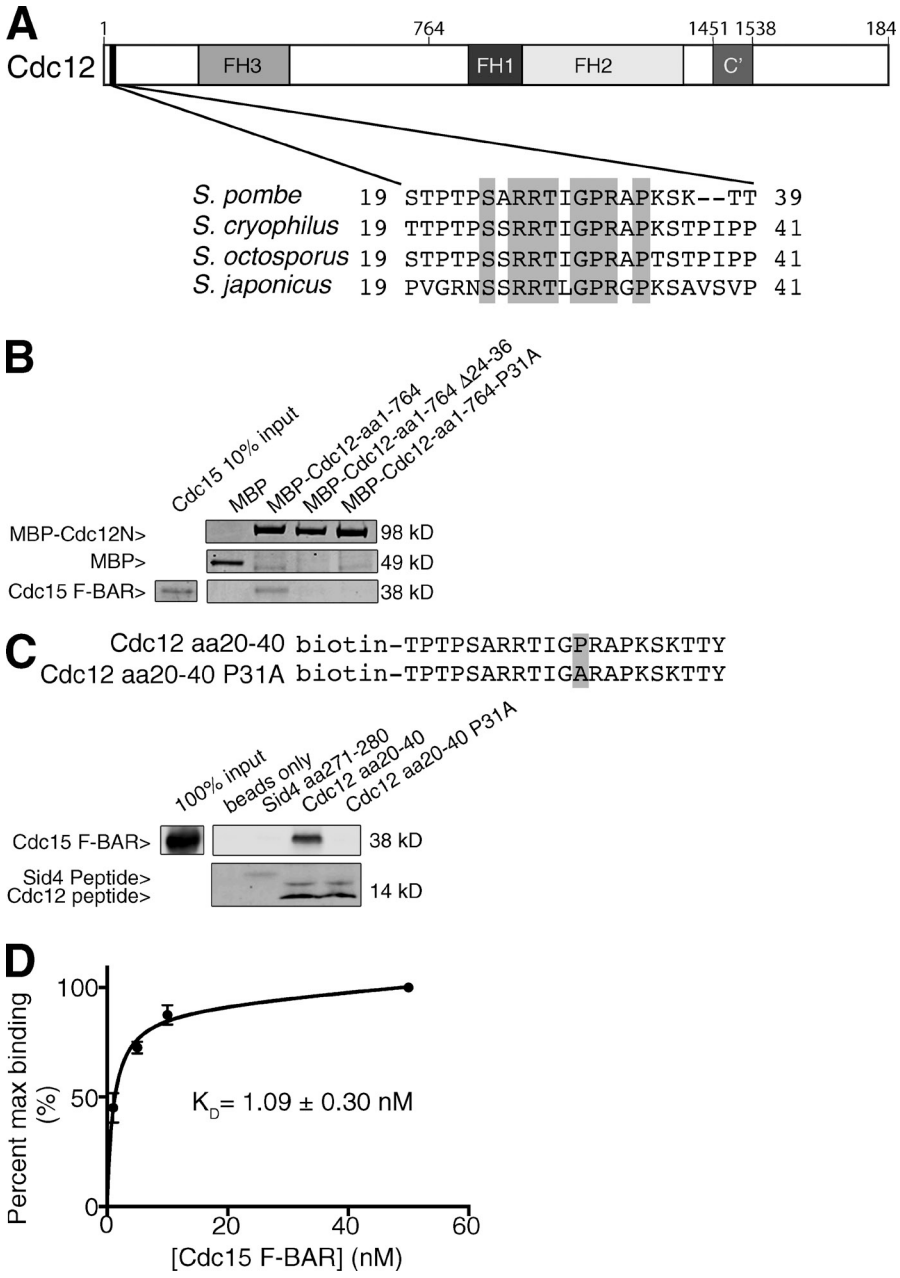

Figure 1. **An N-terminal Cdc12 motif directly interacts with the Cdc15 F-BAR.** (A) A schematic, drawn to scale, of Cdc12 with the relative position of aa 24–36 indicated by the black bar, and other relevant amino acids and domains are indicated. At the bottom, is a ClustalW alignment of Cdc12 (aa 19–39), with sequences from *Schizosaccharomyces cryophilus* (UniProt accession no. S9W3Y3), *Schizosaccharomyces octosporus* (S9PXQ8), and *Schizosaccharomyces japonicus* (B6JV74) Cdc12-related proteins. Shading indicates identical amino acids among all four aligned sequences. (B) In vitro binding assay of bead-bound recombinant MBP, MBP-Cdc12 (aa 1–764), MBP-Cdc12 (aa 1–764)-Δ24–36 or MBP-Cdc12 (aa 1–764)-P31A with recombinant Cdc15 F-BAR (aa 19–312). Samples were washed, resolved by SDS-PAGE, and stained with Coomassie blue. (C, top) Sequence of synthetic Cdc12 peptides with variation in sequence shaded. (bottom) Synthetic peptides conjugated to streptavidin beads were incubated with recombinant Cdc15 F-BAR (aa 19–312). Samples were washed and resolved with SDS-PAGE, and bead-bound proteins were detected by immunoblotting. An unrelated peptide (Sid4-aa 271–280) was used as a negative control. (D) Titration of Cdc12 (aa 20–40) with Cdc15 F-BAR (aa 19–312). Binding assays were performed with increasing concentrations of Cdc15 F-BAR (aa 19–312), and the amount of bound protein was measured. The dissociation constant was determined with least-squares fitting (Prism 6; GraphPad Software). Error bars represent SEM.

2011), it is important to clarify its role in CR assembly. To do so, we defined the Cdc15-binding motif within the Cdc12 N terminus and constructed Cdc12 mutants that cannot interact with Cdc15. Cells lacking the Cdc12–Cdc15 interaction assembled CRs but had reduced Cdc12 in the CR, a delay in the medial accumulation of F-actin and actin-binding proteins, delayed CR formation, and were unable to survive other perturbations to CR assembly. Thus, the Cdc12–Cdc15 interaction is an important contributor to Cdc12 localization and CR formation.

Results and discussion

Cdc12 binds the Cdc15 F-BAR through a conserved N-terminal motif

We previously detected an interaction between Cdc15 and the Cdc12 N terminus that depended on the phosphorylation state of Cdc15 (Carnahan and Gould, 2003; Roberts-Galbraith et al., 2010). The Cdc12–Cdc15 interaction was unprecedented because it involved the F-BAR domain of Cdc15 rather than its SH3 domain (Carnahan and Gould, 2003). Because the first 151 residues of Cdc12 localized GFP to the division site (Yonetani et al., 2008), we examined these amino acids for a candidate Cdc15 interaction motif. Sequence comparison of Cdc12 aa 1–151 with its orthologues in other *Schizosaccharomyces* species revealed one conserved motif (aa 24–36; Fig. 1 A). Deletion of this motif (Δ24–36) or mutation of a conserved proline within it (P31A) resulted in loss of interaction with the Cdc15 F-BAR domain in vitro (Fig. 1 B). A synthetic peptide containing the motif (aa 20–40) bound the Cdc15 F-BAR, whereas mutation of P31 to alanine within the peptide abolished the interaction (Fig. 1 C). Titration binding assays between the Cdc12 peptide and the Cdc15 F-BAR

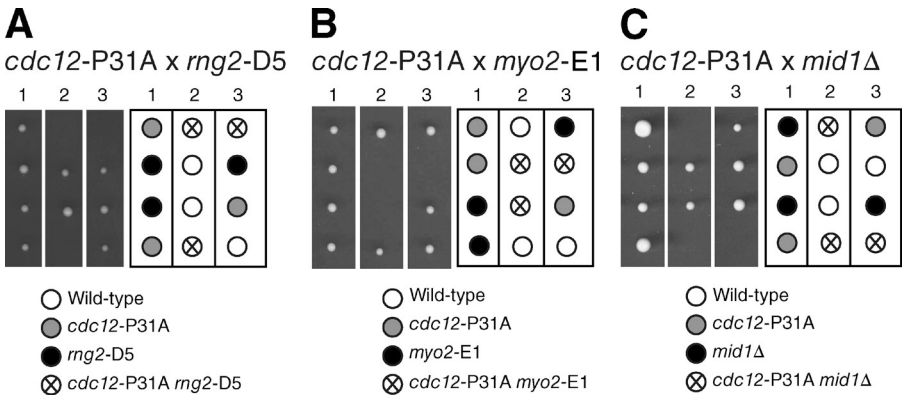

Figure 2. **Genetic interactions of mutant *cdc12*-P31A.** (A–C) Tetrads from *cdc12*-P31A crossed to *rng2*-D5 (A), *myo2*-E1 (B), and *mid1Δ* (C) are shown with a schematic of relevant genotypes.

revealed a dissociation constant of 1.1 nM, indicating a strong affinity (Fig. 1 D). Because Cdc12 is a low abundance protein (Wu and Pollard, 2005), a strong interaction may be necessary to recruit or maintain it at the cell middle. In fact, other protein–protein interactions that promote the localization of other formins are also in the nanomolar affinity range (Brandt et al., 2007; Watanabe et al., 2010). As might be expected from this tight association, Cdc12 (aa 24–36) fused to GFP localized to the division site (Fig. S1), supporting the possibility that this motif participates in directing Cdc12 to the cell middle.

Cells lacking the Cdc12-Cdc15 interaction are prone to cytokinesis failure

To determine the functional consequence of disrupting the Cdc12–Cdc15 interaction, we constructed *cdc12* alleles at the endogenous locus in which the binding motif was mutated or deleted. Although *cdc12*-P31A and *cdc12*-Δ24–36 cells are viable, they displayed synthetic lethal genetic interactions with *rng2*-D5, *myo2*-E1, and *mid1Δ* (Fig. 2, A–C; and Fig. S2, A–C). Myo2, Rng2, and Mid1 contribute to Cdc12 recruitment through a common genetic pathway distinct from Cdc15 (Laporte et al., 2011), and therefore, synthetic lethality likely results from the combined disruption of both Cdc12 recruitment pathways. *cdc12*-P31A and *cdc12*-Δ24–36 did not show a strong genetic interaction with *cdc15*-140 (Fig. S2 D), as would be expected if these alleles disrupt a major Cdc15 pathway during cytokinesis.

Cdc12-Cdc15 interaction is important for normal Cdc12 recruitment

To test whether Cdc12 binding to Cdc15 influences Cdc12 localization to the CR, we tagged wild-type and mutant alleles with a single copy of mNeonGreen (mNG), a brighter and more photostable variant of GFP (Shaner et al., 2013). We compared mutant and wild-type cells in the same field of view using TRITC-conjugated lectin cell wall staining to differentiate between strains (Fig. 3 A). In addition, we used the spindle pole body (SPB) marker Sid4-GFP to define the stages of mitosis based on the distance between spindle poles. At mitotic onset, SPBs separate to opposite sides of the nucleus as the spindle forms, and they maintain a constant distance from one another throughout metaphase and anaphase A of ∼2.5 µm (Hagan, 1998; Nabeshima et al., 1998). We refer to these stages combined as "early mitotic," as only ∼1/9 of cells with constant spindle length are in anaphase A (Nabeshima et al., 1998). SPBs move apart again at the onset of anaphase B. CRs in early mitotic cells had 35–36% less Cdc12-P31A-mNG or Cdc12-Δ24–36-mNG than wild-type Cdc12-mNG, and the amount of mutant Cdc12 did not increase during anaphase B like wild-type Cdc12 (Fig. 3, A and B). However, there was no significant difference in total Cdc12 protein levels in mitotic cells among strains (Fig. 3 C). Thus, Cdc15 helps recruit/maintain Cdc12 at the medial cortex during mitosis. These results also indicate that significantly less CR-associated Cdc12 is sufficient for CR formation, a finding that is in accord with the survival of diploids with a single functional copy of *cdc12*$^+$ (Chang et al., 1997).

Cdc15 also influences Cdc12 localization in abnormal cell cycle situations (Carnahan and Gould, 2003; Roberts-Galbraith et al., 2010). For example, a *cdc15* phosphomutant (*cdc15-S11A*) precociously localizes to the medial cortex when cells are arrested in G2; concomitantly, Cdc12 forms one or two medial cortical spots (Roberts-Galbraith et al., 2010). To test whether this precocious Cdc12 recruitment depends on Cdc15 binding, we visualized *cdc25-22 cdc15-S11A* cells with Cdc12-mNG or Cdc12-P31A-mNG. In contrast to Cdc12-mNG, which localized as bright central dots, Cdc12-P31A-mNG was diffuse in the cytoplasm (Fig. 3, D and E). A Cdc12 mutant lacking the C-terminal oligomerization domain (C′; Cdc12-ΔC′-mNG; Bohnert et al., 2013) formed a central streak rather than focused spots under these conditions, in accord with its lack of self-association (Fig. 3, D and E). However, the double mutant (Cdc12-P31A-ΔC′-mNG) showed diffuse cytoplasmic localization (Fig. 3, D and E), revealing the importance of the Cdc15 association for precocious Cdc12 medial recruitment. Overexpression of *cdc15* also results in the formation of large puncta of Cdc12 (Carnahan and Gould, 2003); this pattern was abolished by the P31A mutation in *cdc12* (Fig. 3 F). Thus, in both normal and abnormal conditions, Cdc15 directs Cdc12's localization via residues 24–36.

Wild-type Cdc12 and Cdc15 localize to the medial cortex independently of F-actin (Wu et al., 2003, 2006). In contrast, N-terminal truncations of Cdc12 (Δ503-*cdc12* and Δ841-*cdc12*) require F-actin for medial recruitment (Coffman et al., 2013). To determine whether abrogation of Cdc15 binding led to F-actin dependence, we treated wild-type and the *cdc12* mutant cells with a high dose of Latrunculin-A (Lat-A) to deplete F-actin. Both Cdc12-mNG and Cdc12-Δ24–36-mNG localized in medial

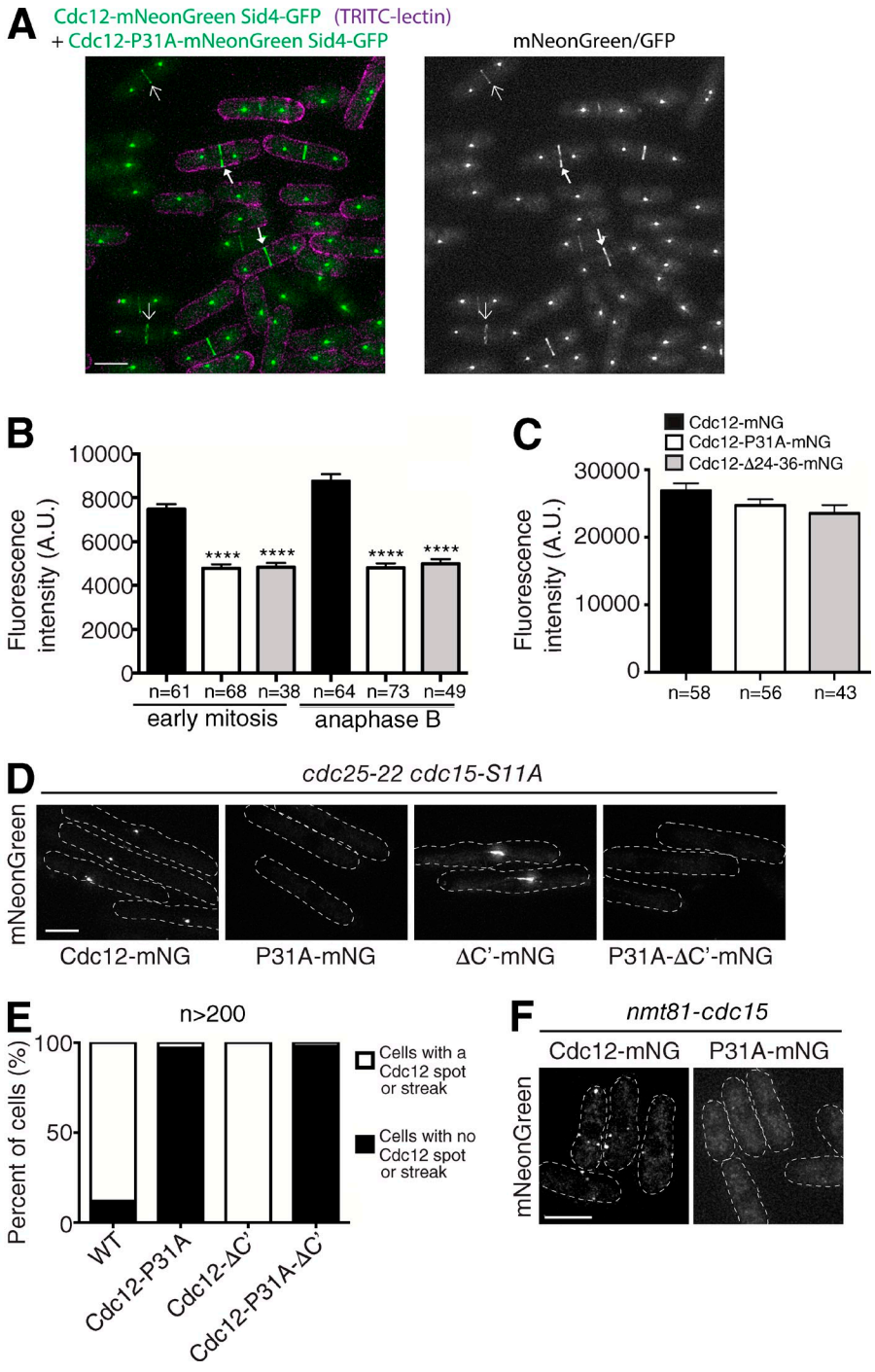

Figure 3. **Cells lacking the Cdc12–Cdc15 interaction accumulate less Cdc12 in the CR.** (A) Live-cell imaging of endogenously tagged Cdc12-mNeonGreen (mNG) or Cdc12-P31A-mNG with Sid4-GFP. The cell wall of wild-type cells was labeled with TRITC-lectin and then mixed with mutant cells before imaging. Thick arrows indicate Cdc12-mNG in the CR, and thin arrows indicate Cdc12-P31A-mNG in the CR. (B) Quantification of fluorescence intensity of the CR from mNG images of cells of the indicated genotypes and cell cycle stage. (C) Quantification of whole cell fluorescence intensity from Cdc12-mNG images of cells with CRs of the indicated genotypes. These measurements were made with stains that do not contain Sid4-GFP (wild type vs. Cdc12-P31A, $P = 0.14$; and wild type vs. Cdc12-Δ24–36, $P = 0.052$). Measurements in the graphs from B and C represent three biological replicates. ****, $P \leq 0.0001$. Error bars represent SEM. (D) Cdc12-mNG localization in *cdc15*-S11A *cdc25*-22 cells shifted to 36°C for 3.5 h. (E) Quantification from D. (F) Localization of Cdc12-mNG in cells overexpressing Cdc15 from the *nmt81* promoter for 20 h at 32°C. Cell outlines are indicated with dotted lines. A.U., arbitrary unit; WT, wild type. Bars, 5 µm.

cortical dots in Lat-A–treated cells, but just as in CRs (Fig. 3, A and B), Cdc12-Δ24–36-mNG was less abundant (Fig. S3 A). Thus, lack of Cdc15 binding does not render Cdc12 localization dependent on F-actin.

Efficient Cdc12 recruitment is important for F-actin accumulation in the CR

Our results indicate that cells lacking the Cdc12–Cdc15 interaction have 33% less Cdc12 at the division site. Assuming that both wild-type and mutant Cdc12 nucleate and elongate F-actin at the same rate, cells lacking the Cdc12–Cdc15 interaction could then take 33% longer to form the F-actin in the CR. Thus, if Cdc12 activity is not otherwise regulated, mutant cells lacking the Cdc12–Cdc15 interaction may still have time to produce sufficient amounts of F-actin for the CR. On the other hand, because F-actin in the CR is rapidly and constantly turned over (Pelham and Chang, 2002), less CR-associated Cdc12 might lead to less F-actin. Therefore, we compared the amount of F-actin in the CR between early mitotic and anaphase B wild-type and mutant cells. There was ∼26% less F-actin, visualized with LifeAct-mCherry, in the CR of *cdc12*-P31A cells compared with wild-type cells during early mitosis (Fig. 4, A and B). However, there was no difference in the amount of F-actin in the CR between the two strains during anaphase B (Fig. 4,

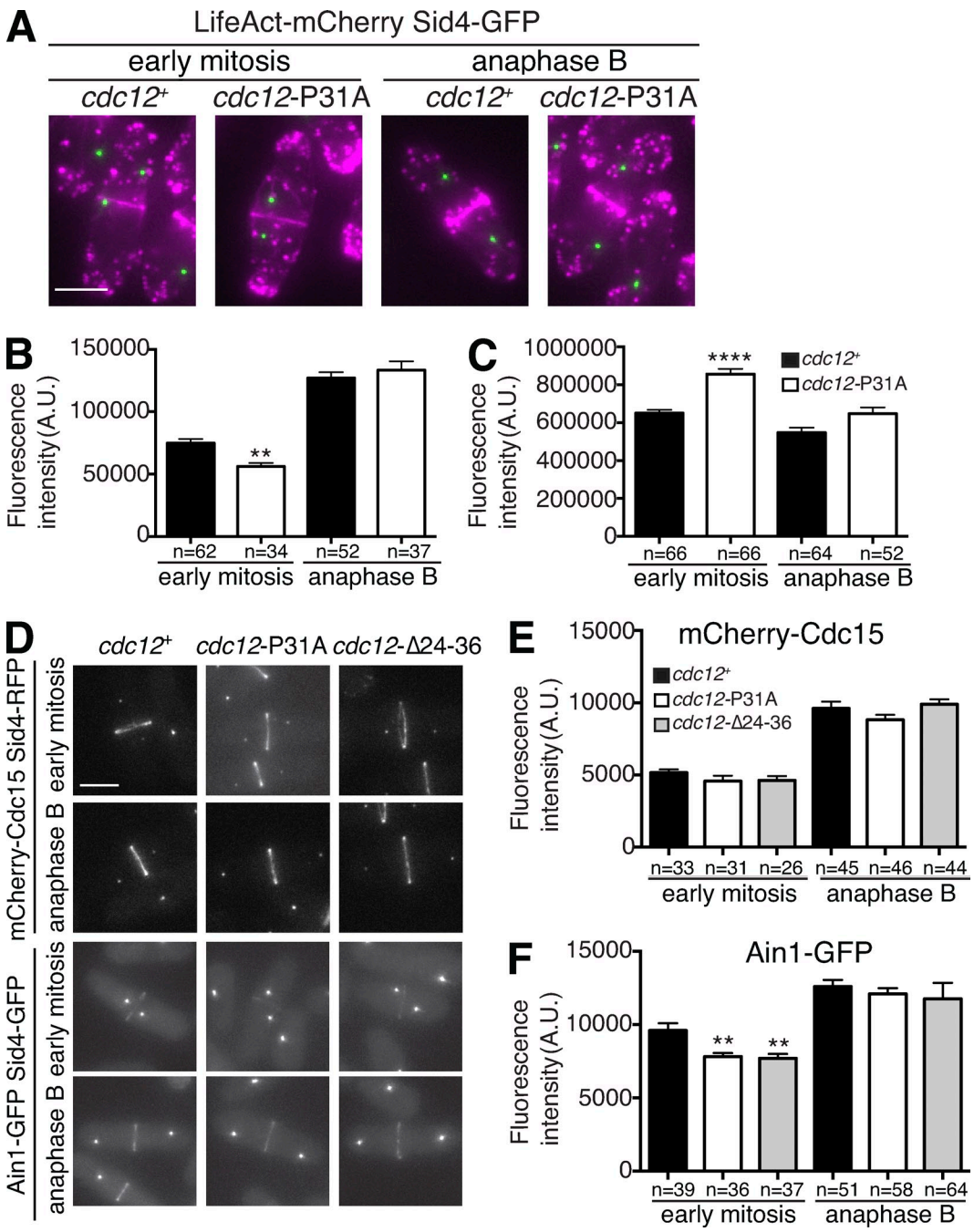

Figure 4. **Cells lacking the Cdc12–Cdc15 interaction accumulate less F-actin in the CR.** (A) Live-cell imaging of *cdc12*$^{+}$ or *cdc12*-P31A cells expressing LifeAct-mCherry Sid4-GFP. (B) Quantification of fluorescence intensity of the CR in cells of the indicated genotypes and cell cycle stage from A. Wild-type anaphase B versus *cdc12*-P31A anaphase B, P = 0.42. (C) Quantification the fluorescence intensity at the cell tips of the indicated genotypes at the indicated cell cycle stage. Wild-type anaphase B versus *cdc12*-P31A anaphase B, P = 0.12. (D) Live-cell imaging of *cdc12*$^{+}$, *cdc12*-P31A, and *cdc12*-Δ24–36 cells expressing endogenously tagged mCherry-Cdc15 or Ain1-GFP with fluorescently tagged Sid4. (E and F) Quantification of fluorescence intensity in cells of the indicated genotypes and cell cycle stage from D. For early mitosis mCherry-Cdc15 wild type versus P31A, P = 0.174, and for wild type versus Δ24–36, P = 0.152. Measurements in the graphs from B, C, E, and F represent three biological replicates. **, P ≤ 0.01; ****, P ≤ 0.0001. Error bars represent SEM. A.U., arbitrary unit. Bars, 5 µm.

A and B). Thus, the mutant Cdc12 produces the same amount of F-actin in the CR as wild type given time. We did not observe a difference in longitudinal F-actin cable number (unpublished data), in accord with Cdc12 specifically producing F-actin for the CR (Chang et al., 1997). Formins compete with the Arp2/3 complex for G-actin, and mutations disrupting formin function have increased F-actin patch density (Burke et al., 2014). As expected, we found an ∼24% increase in fluorescence intensity of actin patches at cell tips in early mitosis but not anaphase B in the mutants compared with wild-type (Fig. 4, A and C) as expected given that less F-actin was incorporated into the CR in the mutant cells.

Although there was less F-actin in the CRs of *cdc12* mutants lacking the Cdc12–Cdc15 interaction in early mitosis, we

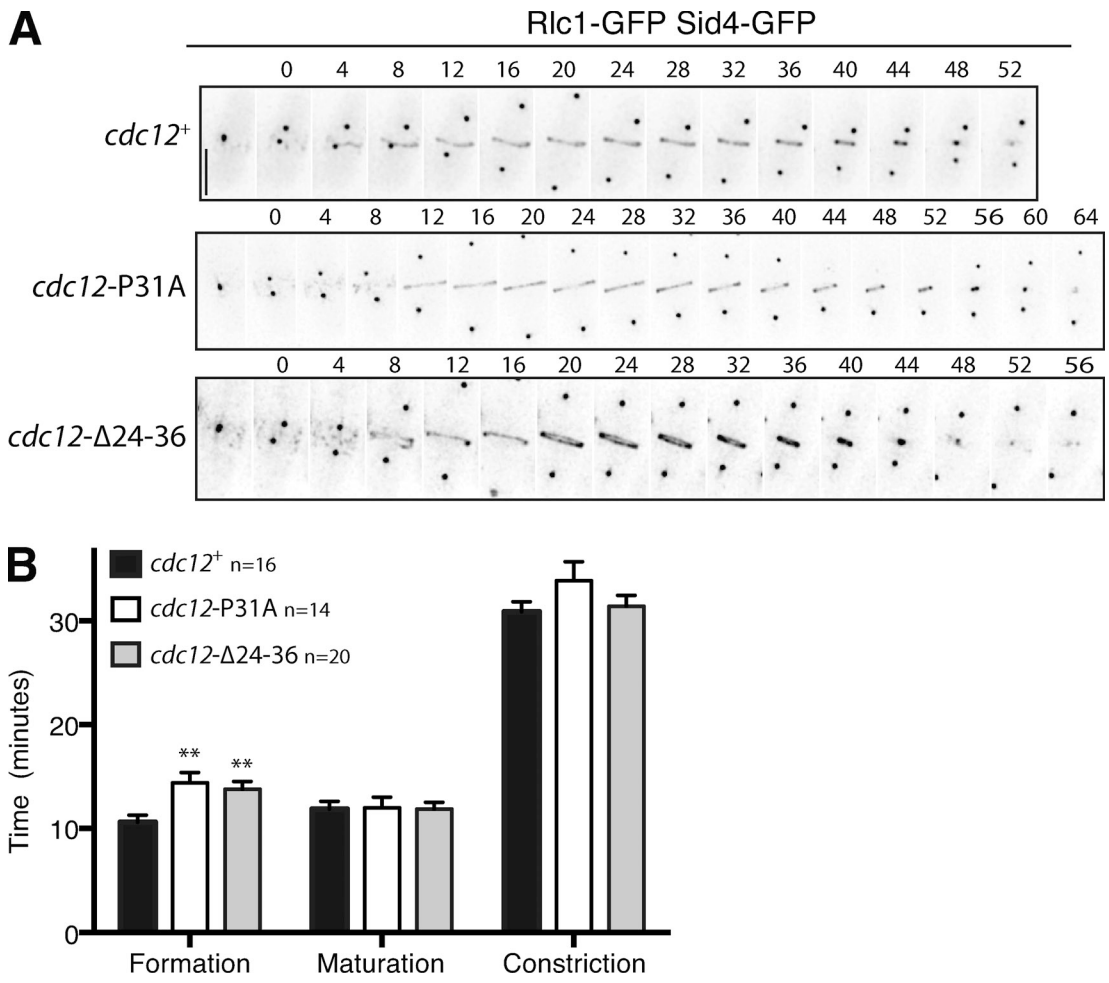

Figure 5. **Cells lacking the Cdc12–Cdc15 interaction exhibit slower CR formation.** (A) Live-cell imaging of *cdc12*$^+$, *cdc12*-P31A, or *cdc12*-Δ24–36 expressing Rlc1-GFP Sid4-GFP during cell division. Images were acquired every 2 min, and representative time points are shown. Bar, 5 µm. (B) Quantification of cytokinesis event timing for each mutant from A. **, P ≤ 0.01. Error bars represent SEM.

expected that proteins targeted there independently of F-actin, such as Cdc15 (Wu et al., 2006) and Myosin II (Naqvi et al., 1999), would not be affected in the mutant cells. Indeed, mCherry-Cdc15 and the myosin light chain Rlc1-GFP did not have altered protein levels in CRs of mutant cells compared with wild type in any mitotic stage (Fig. 4, D and E; and Fig. S3, B and C). In contrast, we anticipated that proteins localizing to the CR in an F-actin–dependent manner would exhibit decreased abundance in the CR of *cdc12* mutants. Indeed, there was an ∼18–19% decrease in Ain1-GFP (an α-actinin protein; Wu et al., 2001) and ∼39% decrease in GFP-Adf1 (a cofilin protein; Nakano et al., 2001) abundance in the CR in the *cdc12* mutants compared with wild type during early mitosis (Fig. 4, D and F; and Fig. S3, B–D). Like F-actin, Ain1-GFP recovered to wild-type levels during anaphase B, although GFP-Adf1 did not. We do not have an explanation for this difference.

The Cdc12–Cdc15 interaction is important during CR formation

Because these results indicated that loss of the Cdc15–Cdc12 interaction adversely affects CR assembly, we used time-lapse microscopy to examine cytokinetic progression. Using Rlc1-GFP and Sid4-GFP as markers for the CR and mitotic progression, respectively, we found that CR formation in *cdc12*-P31A and *cdc12*-Δ24–36 mutants was 26% and 23% slower, respectively, from the time of initial SPB separation compared with wild type (Fig. 5, A and B), in remarkable agreement with the reduction in F-actin. In contrast to some other mutations affecting CR formation (Coffman et al., 2009; Roberts-Galbraith et al., 2010; Tebbs and Pollard, 2013; Wang et al., 2014), we did not observe a compensatory decrease in the amount of time for CR maturation (the time between CR formation and the beginning of CR constriction).

We wondered whether binding to Cdc15 cooperated with previously described regulatory inputs into Cdc12 localization and function. We therefore carefully assessed CR dynamics in *cdc12* mutant cells lacking its oligomerization domain (*cdc12*-ΔC′) and a phosphomutant whose multimerization cannot be regulated by the septation initiation network (SIN; *cdc12*-4A; Bohnert et al., 2013). The latter mutant renders CR assembly completely dependent on Mid1 (Bohnert et al., 2013). Although no changes in CR dynamics were observed in *cdc12*-ΔC′ cells compared with wild type, CR constriction took significantly longer in *cdc12*-4A cells (Fig. S3 E). Next, we assayed CR dynamics in double mutants with *cdc12*-P31A. The phenotypes

reflected the defects of the individual single mutants, and therefore, the mutations are not additive (Fig. S3 E). Thus, Cdc15 and the SIN affect different aspects of Cdc12 function: Cdc15 binding to Cdc12 promotes its medial recruitment, whereas SIN-dependent phosphorylation of Cdc12 controls its oligomerization state that is important later in cytokinesis.

Summary

Although little Cdc12 is required for CR formation, its medial recruitment depends on multiple inputs. Here, we have established that Cdc15 is one of these inputs, contributing to Cdc12 recruitment during mitosis via direct binding. Our findings provide a rationale for why Cdc15 localizes early in the process of CR assembly (Fankhauser et al., 1995) despite its other described roles later in cell division (Wachtler et al., 2006; Vjestica et al., 2008; Roberts-Galbraith et al., 2009, 2010; Arasada and Pollard, 2014). The existence of multiple inputs for formin recruitment occurs in other biological contexts although the details differ (Chesarone et al., 2010). Of the formins with described recruitment pathways, many rely on a combination of intrinsic properties (membrane binding and/or dimerization/multimerization; Bohnert et al., 2013; Rousso et al., 2013) and extrinsic pathways (protein binding partners; Seth et al., 2006; Copeland et al., 2007; Chesarone et al., 2010; Liu et al., 2012). *Homo sapiens* mDia2, for example, requires interactions with both RhoA and Anillin to direct its localization and control its function during cytokinesis (Watanabe et al., 2010). *Saccharomyces cerevisiae* Bni1 localization to the bud neck requires dimerization of its N terminus in combination with two protein-binding domains, one for Rho1 and another for Spa2 (Fujiwara et al., 1998; Liu et al., 2012). Thus, it is likely that still more formins will be found to use a combination of sequence motifs to direct their intracellular localization, and some may be similar to the Cdc12 mechanism.

In the absence of Cdc15 binding, Cdc12 is still recruited for CR formation, likely through other N-terminal interactions with Rng2 and/or Myo2 based on genetic evidence (Laporte et al., 2011) and recent synthetic targeting experiments (Johnson et al., 2014; Tao et al., 2014). To elaborate, precocious targeting of Myo2 or Rng2 to the medial cortex is sufficient for Cdc12 recruitment and vice versa (Tao et al., 2014). Future studies will be aimed at determining the relative importance of various regulatory inputs into Cdc12 recruitment and function. We note that although Cdc15 can promote Cdc12 localization to medial cortical spots during interphase, this is insufficient for Cdc12 activation and the formation of CR F-actin (Fig. 3 D; Roberts-Galbraith et al., 2010). Thus, other interactions and/or protein modifications must promote Cdc12 F-actin nucleation and elongation functions.

Formin Cdc12 recruitment to the cell middle via direct binding to the Cdc15 F-BAR domain provides one of the first examples of a bifunctional F-BAR domain that interacts with a protein partner as well as the membrane. Since our original observation (Carnahan and Gould, 2003), only one other example has emerged (Kostan et al., 2014). Pacsin2, in addition to binding membranes, can interact with F-actin via its F-BAR domain (Qualmann et al., 1999; Kessels et al., 2006; Kostan et al., 2014). However, these two partners of the Pascin2 F-BAR compete to bind the same surface of the domain (Kostan et al., 2014). Although we do not yet know whether Cdc12 competes with membrane for binding to the Cdc15 F-BAR, it is likely that the F-BAR domain binds both simultaneously because both Cdc15–Cdc12 and Cdc15–membrane interactions are restricted to the same narrow time window when Cdc15 is dephosphorylated during mitosis (Wachtler et al., 2006; Roberts-Galbraith et al., 2010). Simultaneous binding would position the N terminus of the formin very close to the plasma membrane to establish a tight bridge between the membrane and CR during cell division. Further study of other F-BAR domains may reveal additional examples of bifunctional binding properties.

Materials and methods

Yeast methods

S. pombe strains (Table S1) were grown in yeast extract (YE). *cdc12*$^{+}$, *cdc12*-P31A, and *cdc12*-Δ24–36 were tagged endogenously at the 3′ end with mNG:kan^{R} or mNG:hyg^{R} using pFA6 cassettes as previously described (Wach et al., 1994; Bähler et al., 1998). The pFA6 plasmid contains a replication origin and amp^{R} for selection in bacteria. mNG, a recently reported GFP derived from the lancelet *Branchiostoma lanceolatum*, was chosen for imaging experiments because of its superior brightness of ∼93 (product of extinction coefficient and quantum yield), compared with ∼34 for EGFP (Shaner et al., 2013; Allele Biotechnology). mNG has an excitation maximum of 506 nm and emission maximum of 517 nm and is currently the brightest known monomeric fluorescent protein in the green–yellow spectrum. A lithium acetate method (Keeney and Boeke, 1994) was used in *S. pombe* tagging transformations, and integration of tags was verified using whole-cell PCR and/or microscopy. Introduction of tagged loci into other genetic backgrounds was accomplished using standard *S. pombe* mating, sporulation, and tetrad dissection techniques. Fusion proteins were expressed from their native promoters at their normal chromosomal locus unless otherwise indicated. Lat-A was used at a final concentration of 100 µM from a 1-mM stock solution in DMSO.

The mNG:kan^{R} and mNG:hyg^{R} pFA6 cassettes were constructed by PCR amplifying the mNG sequence with the PacI restriction site in the forward primer and the Asc1 restriction site in the reverse primer. The sequence was subcloned into the pFA6 vector with the respective resistance cassettes.

To make the endogenous *cdc12*-P31A and *cdc12*-Δ24–36 alleles, a pSK vector (pBluescript backbone) was constructed that contained in the following order 5′ *cdc12* flank including its promoter, full-length *cdc12*$^{+}$, kan^{R} cassette, and 3′ *cdc12* flank (pKG 5431; Bohnert et al., 2013). The *cdc12*-P31A mutation and *cdc12*-Δ24–36 deletion were created with mutagenesis of pKG 5431 by PCR and confirmed with sequencing. The mutant constructs were then released from the vector by digestion with Xba1 and Sac1 and transformed into wild-type *S. pombe* cells using a lithium acetate method (Keeney and Boeke, 1994). G418-resistant cells were selected, and the *cdc12* locus was sequenced to identify transformants containing the desired and correct mutations.

For growth assays, cells were grown to log phase at 25°C in YE, 10 million cells were resuspended in 1 ml of water, and 10-fold serial dilutions were made. 2.5 µl of each dilution was spotted on YE plates, and the plates were incubated at the indicated temperatures.

The GFP-Cdc12 (aa 24–36) fragment was placed under the control of the nmt81 promoter in pREP81 plasmid vector. This construct and a construct with GFP alone were expressed in a wild-type strain. Cells were grown in media containing thiamine and then washed into media without thiamine to induce protein production and grown for 20 h at 32°C before imaging.

Protein expression and purification

Cdc12 (aa 1–764) was cloned into pMAL-2c for expression as a maltose-binding protein (MBP) fusion (Carnahan and Gould, 2003). pMal-2c contains the P_{tac} promoter and amp^{R} gene. Cdc15 F-BAR (aa 19–312) was cloned into pET15b for expression as a 6×His fusion. Proteins were induced in *Escherichia coli* Rosetta2(DE3)pLysS cells with 0.4 mM IPTG overnight at 18°C. Protein was purified on amylose beads (New England Biolabs, Inc.) or cOmplete His-Tag resin (Roche) according to the manufacturer's protocols. Cdc15 (aa 19–312)'s 6×His tag was removed with thrombin protease, and

the protein was further purified on a HiTrap Q SP anion exchange column (GE Healthcare) and concentrated.

In vitro binding

Recombinant proteins conjugated to amylose beads or synthetic biotinylated peptides (5 µg; GenScript) conjugated to streptavidin beads were incubated with recombinant Cdc15 F-BAR for 1 h at 4°C in binding buffer (50 mM Tris-HCl, pH 7.0, 250 mM NaCl, 2 mM EDTA, and 0.1% NP-40). For Fig. 2 A, 0.3 µM MBP-Cdc12N was incubated with 30 nM Cdc15 F-BAR. For Fig. 2 C, 30 nM peptide was incubated with 30 nM Cdc15 F-BAR. For the titration binding assay, 30 nM Cdc12 (aa 20–40) was added for all concentrations of Cdc15 F-BAR (1, 5, 10, and 50 nM). After extensive washing in binding buffer, samples were resolved by SDS-PAGE for Coomassie blue staining or Western blot analysis. For detection of biotinylated peptides, a streptavidin infrared dye was used (LI-COR Biosciences). The Cdc15 F-BAR was detected using a rabbit polyclonal antibody raised against GST-Cdc15 (aa 1–405; Roberts-Galbraith et al., 2009).

Microscopy

Live-cell images of *S. pombe* cells were acquired using a Personal DeltaVision (Applied Precision) that includes a microscope (IX71; Olympus), 60× NA 1.42 Plan Apochromat and 100× NA 1.40 U Plan S Apochromat objectives, fixed and live-cell filter wheels, a camera (CoolSNAP HQ2; Photometrics), and softWoRx imaging software (Applied Precision). Images were acquired at 25–29°C, and cells were imaged in YE media. Images in figures were maximum intensity projections of z sections spaced at 0.2–0.5 µm. Images used for quantification were not deconvolved. Other images not used for fluorescence quantification were deconvolved with 10 iterations.

Time-lapse imaging was performed on cells in log phase using a microfluidics perfusion system (CellASIC ONIX; EMD Millipore). Cells were loaded into Y04C plates for 5 s at 8 psi, and YE liquid media were flowed into the chamber at 5 psi throughout imaging.

Intensity measurements were made with ImageJ software (National Institutes of Health). For all intensity measurements, the background was subtracted by creating a region of interest (ROI) in the same image where there were no cells (Waters, 2009). The area of the background was divided by the raw intensity of the background, which was multiplied by the area of the ROI. This number was subtracted from the raw integrated intensity of that ROI (Waters, 2009). For CR intensity quantification, an ROI was drawn around the CR and measured for raw integrated density, and for whole cell intensity quantification, an ROI was drawn around the entire cell.

To compare populations of cells for all genotypes, cells were imaged on the same day with the same microscope parameters. In addition, to compare two populations of cells within the same field of view, one population was incubated with fluorescently conjugated lectin (Sigma-Aldrich), which labels cell walls. Specifically, 1 µl of a 5-mg/ml stock of TRITC-lectin in water was added to 1 ml of cells for a final concentration of 5 µg/ml. Cells were then incubated for 10 min at room temperature, washed three times, and resuspended in media. The lectin-labeled cell population and unlabeled cell population were mixed 1:1 immediately before imaging. The reciprocal labeling of populations was also performed to account for any bleed through. The fluorescence intensity of the cell tips was quantified by using the exact same size circle, 3.5 µm in diameter, placed at the tip of each cell end and then subtracting background (Burke et al., 2014).

Online supplemental material

Fig. S1 shows that Cdc12 (aa 24–36) fused to GFP localizes to the cell division site. Fig. S2 shows that the *cdc12*-Δ24–36 allele is synthetically lethal with *rng2*-D5, *myo2*-E1, and *mid1Δ*, whereas *cdc12*-P31A and *cdc12*-Δ24–36 do not have a significant genetic interaction with *cdc15*-140. Fig. S3 shows that Cdc12 lacking the Cdc12–Cdc15 interaction localizes independently of F-actin to the CR. Table S1 lists the genotypes of all strains used in this study. Online supplemental material is available at http://www.jcb.org/cgi/content/full/jcb.201411097/DC1.

We thank Christine Jones, MariaSanta Mangione, Rodrigo Guillen, Quanwen Jin, and especially Dr. Janel Beckley for helpful discussions and critical reading and editing of this manuscript.

We are grateful for the following support: National Institutes of Health grants GM101035 (to K.L. Gould) and T32-CA119925 (for K.A. Bohnert) and American Heart Association grant 14PRE19740000 (to A.H. Willet).

The authors declare no competing financial interests.

Submitted: 21 November 2014
Accepted: 9 January 2015

References

Arai, R., and I. Mabuchi. 2002. F-actin ring formation and the role of F-actin cables in the fission yeast *Schizosaccharomyces pombe*. *J. Cell Sci.* 115:887–898.

Arasada, R., and T.D. Pollard. 2014. Contractile ring stability in *S. pombe* depends on F-BAR protein Cdc15p and Bgs1p transport from the Golgi complex. *Cell Reports*. 8:1533–1544. http://dx.doi.org/10.1016/j.celrep.2014.07.048

Bähler, J., J.Q. Wu, M.S. Longtine, N.G. Shah, A. McKenzie III, A.B. Steever, A. Wach, P. Philippsen, and J.R. Pringle. 1998. Heterologous modules for efficient and versatile PCR-based gene targeting in *Schizosaccharomyces pombe*. *Yeast*. 14:943–951. http://dx.doi.org/10.1002/(SICI)1097-0061(199807)14:10<943::AID-YEA292>3.0.CO;2-Y

Balasubramanian, M.K., D. McCollum, L. Chang, K.C. Wong, N.I. Naqvi, X. He, S. Sazer, and K.L. Gould. 1998. Isolation and characterization of new fission yeast cytokinesis mutants. *Genetics*. 149:1265–1275.

Bohnert, K.A., A.P. Grzegorzewska, A.H. Willet, C.W. Vander Kooi, D.R. Kovar, and K.L. Gould. 2013. SIN-dependent phosphoinhibition of formin multimerization controls fission yeast cytokinesis. *Genes Dev.* 27:2164–2177. http://dx.doi.org/10.1101/gad.224154.113

Brandt, D.T., S. Marion, G. Griffiths, T. Watanabe, K. Kaibuchi, and R. Grosse. 2007. Dia1 and IQGAP1 interact in cell migration and phagocytic cup formation. *J. Cell Biol.* 178:193–200. http://dx.doi.org/10.1083/jcb.200612071

Burke, T.A., J.R. Christensen, E. Barone, C. Suarez, V. Sirotkin, and D.R. Kovar. 2014. Homeostatic actin cytoskeleton networks are regulated by assembly factor competition for monomers. *Curr. Biol.* 24:579–585. http://dx.doi.org/10.1016/j.cub.2014.01.072

Carnahan, R.H., and K.L. Gould. 2003. The PCH family protein, Cdc15p, recruits two F-actin nucleation pathways to coordinate cytokinetic actin ring formation in *Schizosaccharomyces pombe*. *J. Cell Biol.* 162:851–862. http://dx.doi.org/10.1083/jcb.200305012

Chang, F., A. Woollard, and P. Nurse. 1996. Isolation and characterization of fission yeast mutants defective in the assembly and placement of the contractile actin ring. *J. Cell Sci.* 109:131–142.

Chang, F., D. Drubin, and P. Nurse. 1997. cdc12p, a protein required for cytokinesis in fission yeast, is a component of the cell division ring and interacts with profilin. *J. Cell Biol.* 137:169–182. http://dx.doi.org/10.1083/jcb.137.1.169

Chesarone, M.A., A.G. DuPage, and B.L. Goode. 2010. Unleashing formins to remodel the actin and microtubule cytoskeletons. *Nat. Rev. Mol. Cell Biol.* 11:62–74. http://dx.doi.org/10.1038/nrm2816

Coffman, V.C., A.H. Nile, I.J. Lee, H. Liu, and J.Q. Wu. 2009. Roles of formin nodes and myosin motor activity in Mid1p-dependent contractile-ring assembly during fission yeast cytokinesis. *Mol. Biol. Cell*. 20:5195–5210. http://dx.doi.org/10.1091/mbc.E09-05-0428

Coffman, V.C., J.A. Sees, D.R. Kovar, and J.Q. Wu. 2013. The formins Cdc12 and For3 cooperate during contractile ring assembly in cytokinesis. *J. Cell Biol.* 203:101–114. http://dx.doi.org/10.1083/jcb.201305022

Copeland, S.J., B.J. Green, S. Burchat, G.A. Papalia, D. Banner, and J.W. Copeland. 2007. The diaphanous inhibitory domain/diaphanous autoregulatory domain interaction is able to mediate heterodimerization between mDia1 and mDia2. *J. Biol. Chem.* 282:30120–30130. http://dx.doi.org/10.1074/jbc.M703834200

Fankhauser, C., A. Reymond, L. Cerutti, S. Utzig, K. Hofmann, and V. Simanis. 1995. The *S. pombe* cdc15 gene is a key element in the reorganization of F-actin at mitosis. *Cell*. 82:435–444. http://dx.doi.org/10.1016/0092-8674(95)90432-8

Fujiwara, T., K. Tanaka, A. Mino, M. Kikyo, K. Takahashi, K. Shimizu, and Y. Takai. 1998. Rho1p-Bni1p-Spa2p interactions: implication in localization of Bni1p at the bud site and regulation of the actin cytoskeleton in *Saccharomyces cerevisiae*. *Mol. Biol. Cell*. 9:1221–1233. http://dx.doi.org/10.1091/mbc.9.5.1221

Hachet, O., and V. Simanis. 2008. Mid1p/anillin and the septation initiation network orchestrate contractile ring assembly for cytokinesis. *Genes Dev.* 22:3205–3216. http://dx.doi.org/10.1101/gad.1697208

Hagan, I.M. 1998. The fission yeast microtubule cytoskeleton. *J. Cell Sci.* 111:1603–1612.

Johnson, M., D.A. East, and D.P. Mulvihill. 2014. Formins determine the functional properties of actin filaments in yeast. *Curr. Biol.* 24:1525–1530. http://dx.doi.org/10.1016/j.cub.2014.05.034

Keeney, J.B., and J.D. Boeke. 1994. Efficient targeted integration at leu1-32 and ura4-294 in *Schizosaccharomyces pombe*. *Genetics*. 136:849–856.

Kessels, M.M., J. Dong, W. Leibig, P. Westermann, and B. Qualmann. 2006. Complexes of syndapin II with dynamin II promote vesicle formation at the trans-Golgi network. *J. Cell Sci.* 119:1504–1516. http://dx.doi.org/10.1242/jcs.02877

Kostan, J., U. Salzer, A. Orlova, I. Törö, V. Hodnik, Y. Senju, J. Zou, C. Schreiner, J. Steiner, J. Meriläinen, et al. 2014. Direct interaction of actin filaments with F-BAR protein pacsin2. *EMBO Rep.* 15:1154–1162. http://dx.doi.org/10.15252/embr.201439267

Kovar, D.R., and T.D. Pollard. 2004. Progressing actin: Formin as a processive elongation machine. *Nat. Cell Biol.* 6:1158–1159. http://dx.doi.org/10.1038/ncb1204-1158

Kovar, D.R., J.R. Kuhn, A.L. Tichy, and T.D. Pollard. 2003. The fission yeast cytokinesis formin Cdc12p is a barbed end actin filament capping protein gated by profilin. *J. Cell Biol.* 161:875–887. http://dx.doi.org/10.1083/jcb.200211078

Laporte, D., V.C. Coffman, I.J. Lee, and J.Q. Wu. 2011. Assembly and architecture of precursor nodes during fission yeast cytokinesis. *J. Cell Biol.* 192:1005–1021. http://dx.doi.org/10.1083/jcb.201008171

Liu, W., F.H. Santiago-Tirado, and A. Bretscher. 2012. Yeast formin Bni1p has multiple localization regions that function in polarized growth and spindle orientation. *Mol. Biol. Cell*. 23:412–422. http://dx.doi.org/10.1091/mbc.E11-07-0631

Nabeshima, K., T. Nakagawa, A.F. Straight, A. Murray, Y. Chikashige, Y.M. Yamashita, Y. Hiraoka, and M. Yanagida. 1998. Dynamics of centromeres during metaphase-anaphase transition in fission yeast: Dis1 is implicated in force balance in metaphase bipolar spindle. *Mol. Biol. Cell*. 9:3211–3225. http://dx.doi.org/10.1091/mbc.9.11.3211

Nakano, K., K. Satoh, A. Morimatsu, M. Ohnuma, and I. Mabuchi. 2001. Interactions among a fimbrin, a capping protein, and an actin-depolymerizing factor in organization of the fission yeast actin cytoskeleton. *Mol. Biol. Cell*. 12:3515–3526. http://dx.doi.org/10.1091/mbc.12.11.3515

Naqvi, N.I., K. Eng, K.L. Gould, and M.K. Balasubramanian. 1999. Evidence for F-actin-dependent and -independent mechanisms involved in assembly and stability of the medial actomyosin ring in fission yeast. *EMBO J.* 18:854–862. http://dx.doi.org/10.1093/emboj/18.4.854

Nurse, P., P. Thuriaux, and K. Nasmyth. 1976. Genetic control of the cell division cycle in the fission yeast *Schizosaccharomyces pombe*. *Mol. Gen. Genet.* 146:167–178. http://dx.doi.org/10.1007/BF00268085

Pelham, R.J., and F. Chang. 2002. Actin dynamics in the contractile ring during cytokinesis in fission yeast. *Nature*. 419:82–86. http://dx.doi.org/10.1038/nature00999

Qualmann, B., J. Roos, P.J. DiGregorio, and R.B. Kelly. 1999. Syndapin I, a synaptic dynamin-binding protein that associates with the neural Wiskott-Aldrich syndrome protein. *Mol. Biol. Cell*. 10:501–513. http://dx.doi.org/10.1091/mbc.10.2.501

Roberts-Galbraith, R.H., and K.L. Gould. 2010. Setting the F-BAR: functions and regulation of the F-BAR protein family. *Cell Cycle*. 9:4091–4097. http://dx.doi.org/10.4161/cc.9.20.13587

Roberts-Galbraith, R.H., J.S. Chen, J. Wang, and K.L. Gould. 2009. The SH3 domains of two PCH family members cooperate in assembly of the *Schizosaccharomyces pombe* contractile ring. *J. Cell Biol.* 184:113–127. http://dx.doi.org/10.1083/jcb.200806044

Roberts-Galbraith, R.H., M.D. Ohi, B.A. Ballif, J.S. Chen, I. McLeod, W.H. McDonald, S.P. Gygi, J.R. Yates III, and K.L. Gould. 2010. Dephosphorylation of F-BAR protein Cdc15 modulates its conformation and stimulates its scaffolding activity at the cell division site. *Mol. Cell*. 39:86–99. http://dx.doi.org/10.1016/j.molcel.2010.06.012

Rousso, T., A.M. Shewan, K.E. Mostov, E.D. Schejter, and B.Z. Shilo. 2013. Apical targeting of the formin Diaphanous in *Drosophila* tubular epithelia. *eLife*. 2:e00666. http://dx.doi.org/10.7554/eLife.00666

Seth, A., C. Otomo, and M.K. Rosen. 2006. Autoinhibition regulates cellular localization and actin assembly activity of the diaphanous-related formins FRLα and mDia1. *J. Cell Biol.* 174:701–713. http://dx.doi.org/10.1083/jcb.200605006

Shaner, N.C., G.G. Lambert, A. Chammas, Y. Ni, P.J. Cranfill, M.A. Baird, B.R. Sell, J.R. Allen, R.N. Day, M. Israelsson, et al. 2013. A bright monomeric green fluorescent protein derived from *Branchiostoma lanceolatum*. *Nat. Methods*. 10:407–409. http://dx.doi.org/10.1038/nmeth.2413

Tao, E.Y., M. Calvert, and M.K. Balasubramanian. 2014. Rewiring Mid1p-independent medial division in fission yeast. *Curr. Biol.* 24:2181–2188. http://dx.doi.org/10.1016/j.cub.2014.07.074

Tebbs, I.R., and T.D. Pollard. 2013. Separate roles of IQGAP Rng2p in forming and constricting the *Schizosaccharomyces pombe* cytokinetic contractile ring. *Mol. Biol. Cell*. 24:1904–1917. http://dx.doi.org/10.1091/mbc.E12-10-0775

Tsujita, K., S. Suetsugu, N. Sasaki, M. Furutani, T. Oikawa, and T. Takenawa. 2006. Coordination between the actin cytoskeleton and membrane deformation by a novel membrane tubulation domain of PCH proteins is involved in endocytosis. *J. Cell Biol.* 172:269–279. http://dx.doi.org/10.1083/jcb.200508091

Vjestica, A., X.Z. Tang, and S. Oliferenko. 2008. The actomyosin ring recruits early secretory compartments to the division site in fission yeast. *Mol. Biol. Cell*. 19:1125–1138. http://dx.doi.org/10.1091/mbc.E07-07-0663

Wach, A., A. Brachat, R. Pöhlmann, and P. Philippsen. 1994. New heterologous modules for classical or PCR-based gene disruptions in *Saccharomyces cerevisiae. Yeast*. 10:1793–1808. http://dx.doi.org/10.1002/yea.320101310

Wachtler, V., Y. Huang, J. Karagiannis, and M.K. Balasubramanian. 2006. Cell cycle-dependent roles for the FCH-domain protein Cdc15p in formation of the actomyosin ring in *Schizosaccharomyces pombe*. *Mol. Biol. Cell*. 17:3254–3266. http://dx.doi.org/10.1091/mbc.E05-11-1086

Wang, N., L. Lo Presti, Y.H. Zhu, M. Kang, Z. Wu, S.G. Martin, and J.Q. Wu. 2014. The novel proteins Rng8 and Rng9 regulate the myosin-V Myo51 during fission yeast cytokinesis. *J. Cell Biol.* 205:357–375. http://dx.doi.org/10.1083/jcb.201308146

Watanabe, S., K. Okawa, T. Miki, S. Sakamoto, T. Morinaga, K. Segawa, T. Arakawa, M. Kinoshita, T. Ishizaki, and S. Narumiya. 2010. Rho and anillin-dependent control of mDia2 localization and function in cytokinesis. *Mol. Biol. Cell*. 21:3193–3204. http://dx.doi.org/10.1091/mbc.E10-04-0324

Waters, J.C. 2009. Accuracy and precision in quantitative fluorescence microscopy. *J. Cell Biol.* 185:1135–1148. http://dx.doi.org/10.1083/jcb.200903097

Wu, J.Q., and T.D. Pollard. 2005. Counting cytokinesis proteins globally and locally in fission yeast. *Science*. 310:310–314. http://dx.doi.org/10.1126/science.1113230

Wu, J.Q., J. Bähler, and J.R. Pringle. 2001. Roles of a fimbrin and an α-actinin-like protein in fission yeast cell polarization and cytokinesis. *Mol. Biol. Cell*. 12:1061–1077. http://dx.doi.org/10.1091/mbc.12.4.1061

Wu, J.Q., J.R. Kuhn, D.R. Kovar, and T.D. Pollard. 2003. Spatial and temporal pathway for assembly and constriction of the contractile ring in fission yeast cytokinesis. *Dev. Cell*. 5:723–734. http://dx.doi.org/10.1016/S1534-5807(03)00324-1

Wu, J.Q., V. Sirotkin, D.R. Kovar, M. Lord, C.C. Beltzner, J.R. Kuhn, and T.D. Pollard. 2006. Assembly of the cytokinetic contractile ring from a broad band of nodes in fission yeast. *J. Cell Biol.* 174:391–402. http://dx.doi.org/10.1083/jcb.200602032

Yonetani, A., R.J. Lustig, J.B. Moseley, T. Takeda, B.L. Goode, and F. Chang. 2008. Regulation and targeting of the fission yeast formin cdc12p in cytokinesis. *Mol. Biol. Cell*. 19:2208–2219. http://dx.doi.org/10.1091/mbc.E07-07-0731